Visualisation of the Potential Energy Surface

Luke Abraham

(Dated: 1st June 2004)

In this talk I will a brief introduction to one of the methods used to visualise the potential energy surface of a multi-dimensional structure.

I. THE ENERGY LANDSCAPE

Although the potential energy surface of a one- or two-dimensional problem is very easy to visualise, as the number of dimensions increase it is much hard to visualise. Figure 1 shows a simple one-dimensional example.

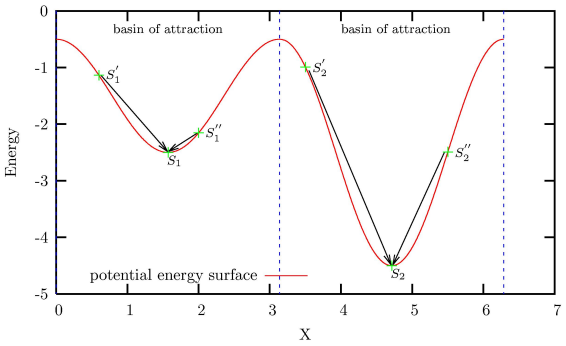

FIG. 1: 1D PES with basins of attraction

Figure 2 shows a two-dimensional example.

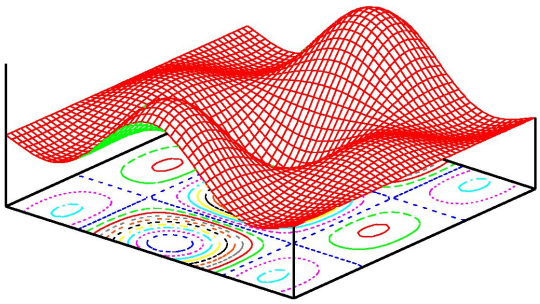

FIG. 2: 2D PES with contours

Problems then arise when more dimensions are added. When dealing with cluster, there are 3N dimensional variables, so even for a two atom cluster, visualising the PES becomes problematic. Another way of describing the energy landscape is required.

II. DISCONNECTIVITY GRAPHS

A. How to form Disconnectivity Graphs

Before giving some example of the use of disconnectivity graphs, I will first explain how to form them.

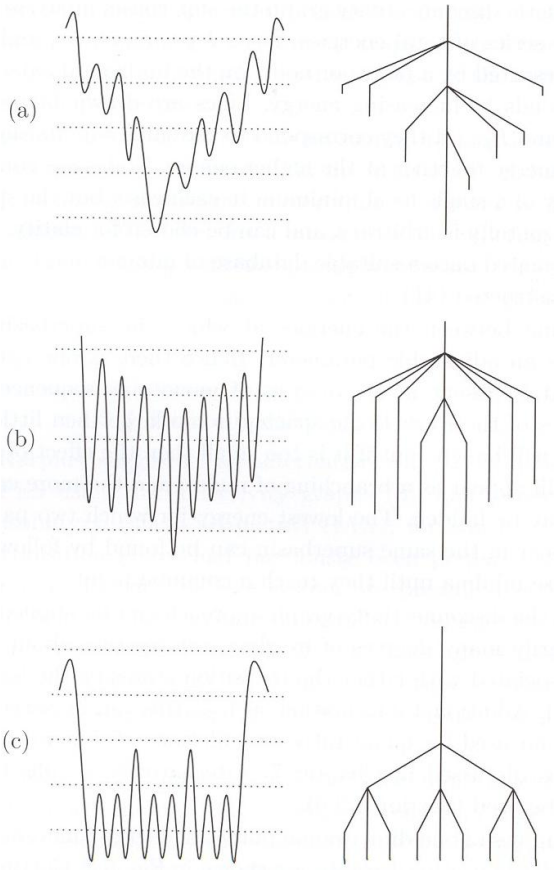

FIG. 3: 1D disconnectivity graphs [5]

Figure 3 shows how the disconnectivity graphs are formed in a 1D example.

At a given energy E, the minima can be classified into disjoint sets, or 'superbasins' if they are connected by pathways or intervening minima, where the energy never exceeds E. Two minima are in different sets if the highest energy transitions state (a local maxima) or lowest energy pathway between them exceeds E. If more than one path connects two minima (not possible in the 1D case) only the lowest energy path is considered in constructing the superbasin. As E is raised more and more minima become accessible and eventu-

ally only one superbasin will remain, containing all the minima (assuming there are no infinite barriers in the PES).

To form the disconnectivity graph, analysis is done at a discrete series of energies, $E_1 > E_2 > E_3$... and each superbasin is represented by a point (or node) on the horizontal axis, with the vertical axis corresponding to increasing energy. Lines are drawn between nodes if they correspond with the same superbasin at higher energy, and nodes are continued down to the energy of a local minimum in each case.

An example of a disconnectivity graph, for the Lennard-Jones 13 atoms cluster is shown in figure 4. This graph shows all 1467 local minima.

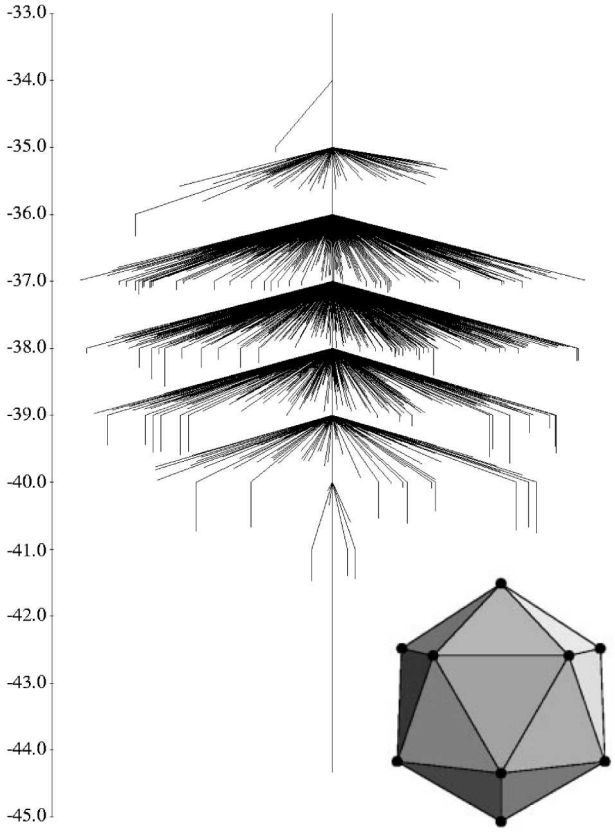

FIG. 4: Disconnectivity Graph for N=13 Lennard-Jones cluster [1]

Figure 4 has the ideal funnel shape for a problem of this type. There is a central stem which leads to the global minimum, which then has branches sprouting from it. In this case 99% of the minima are within two rearrangements of global minimum, and none are more than three rearrangements.

However, forming disconnectivity graphs is not straightforward. A database of structures must first be generated, which not only contains local minima, but also the transition states between minima. In the case of figure 4 a database containing all minima and transition states was able to be generated, but for larger systems it is not practical to compute and store all the minima and transition states. The density of lines on the graph would also become unfeasible. As the system size increases the graphs then have to focus down to the lower energy regions of the PES, which means that inevitably some of the information is lost.

III. LENNARD-JONES CLUSTERS AND OTHER SYSTEMS

The $N = 13$ is the first magic number in the Lennard-Jones clusters, which form around Mackay Icosahedra, which have magic numbers at $N = 13,\ 55,\ 147,\ 309,\ \ldots$ etc. For clusters of other sizes structures based on incomplete Mackay icosahedra are usually also the minimum energy structure, however, in some circumstances, structures based around other forms are the minimum.

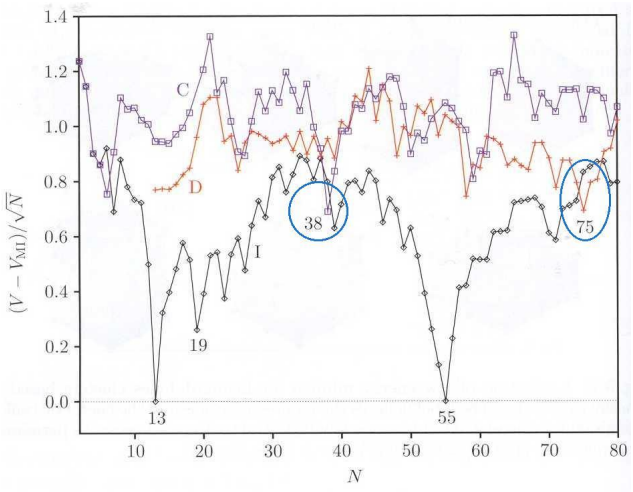

FIG. 5: Comparison of minimum energy with structure type for Lennard-Jones clusters [5]

The graph in figure 5 compares the energies of minimum energy forms of icosahedral (I), decahedral (D) and close-packed (C) cluster types. The zero energy is V_{MI}, which is a function fitted to the energies of the first four Mackay icosahedra: $V_{MI} = -2.3476 - 5.4633N^{1/3} - 14.8814N^{2/3} - 8.5699N$. The areas circled have minimum energy structures of the FCC truncated octahedron for the $N = 38$ cluster, with the $75 \leq N \leq 77$ based on the Marks decahedron. Figure 6 shows the three types of structure.

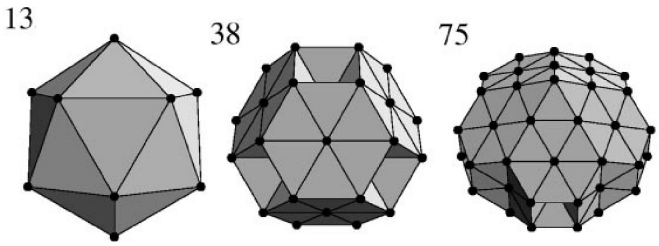

FIG. 6: Structures of the $N = 13,\ 38,$ and 75 Lennard-Jones clusters [1]

Because the global minimum is no longer based on a Mackay icosahedra, the disconnectivity graphs have a “double funnel” structure.

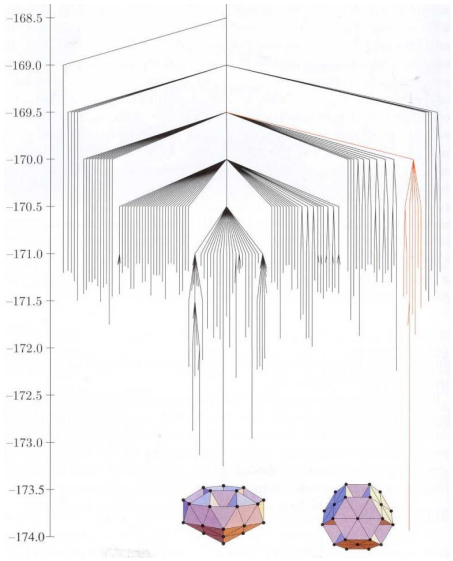

FIG. 7: Disconnectivity graph for $N = 38$ cluster [5]

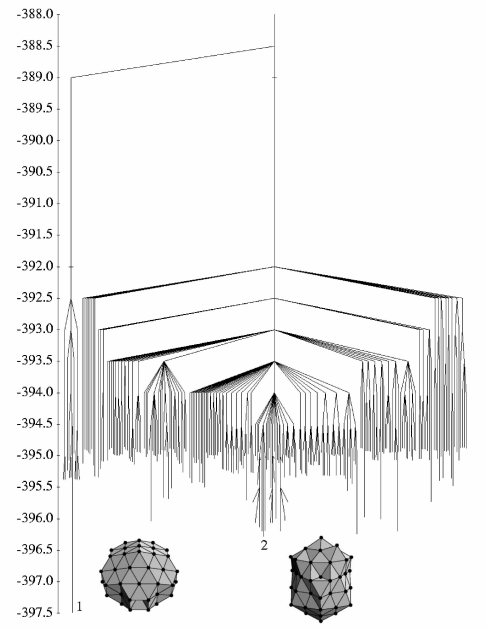

FIG. 8: Disconnectivity graph for $N = 75$ cluster [1]

Figure 7 shows the disconnectivity graph for the $N = 38$ cluster, where the double funnel can be clearly seen. It is even more evident in figure 8. Clusters with $N = 98$ and $102 \leq N \leq 104$ also have non Mackay minima. The $102 \leq N \leq 104$ also based around the Marks decahedron, and the the $N = 98$ around the Leary tetrahedron.

Molecules can also be described using disconnectivity graphs. Figure 9 is one such example, showing the model tetrapeptide Ac(ala)$_3$NHMe.

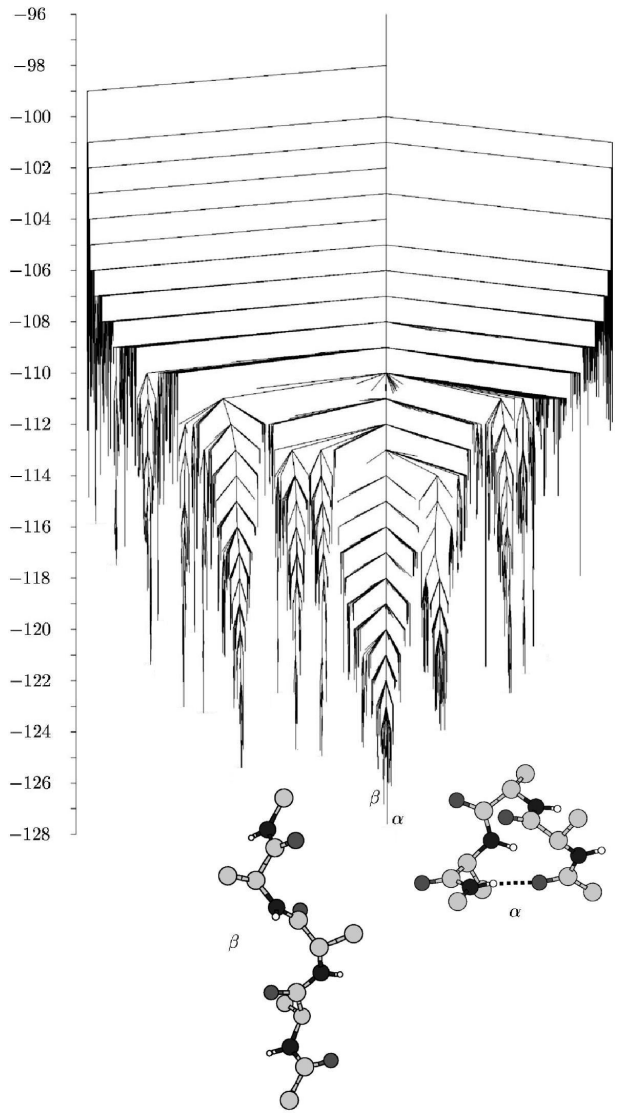

FIG. 9: Disconnectivity graph for Ac(ala)$_3$NHMe, energy in kcal/mol. The two lowest energy structures, the α-turn and the β-strand are shown.[2]

Disconnectivity graphs need not just be formed for systems such as clusters or molecules. Figure 10 is the disconnectivity graph for Stillinger-Weber silicon, with 216 atoms in the supercell, where the branches indicate defects. In this case (and with most cases where not all the minima and transition states are shown) the region of the PES described by the database (and hence the diconnectivity graph) should be representative of the region explored by the system under experimental conditions.

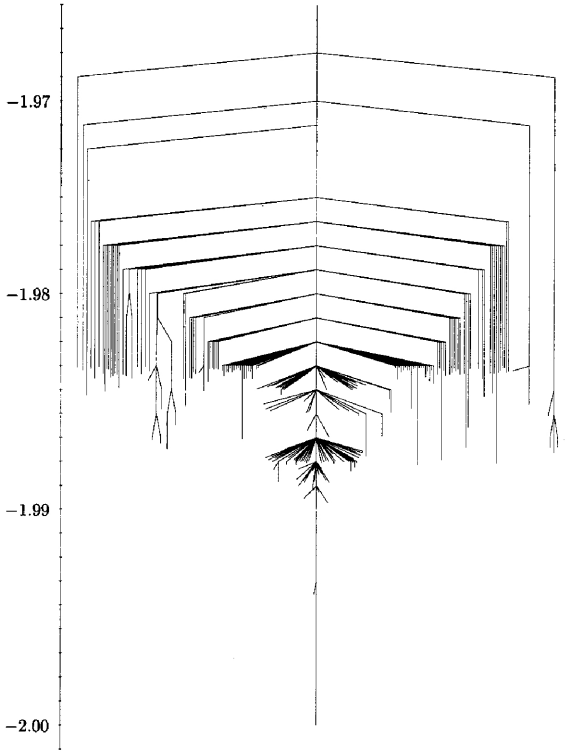

FIG. 10: Disconnectivity graph for silicon. Energies are in ϵ per atom, where $\epsilon = 2.1682$eV.[3]

IV. APPLICATIONS

So, why should we form these large databases and disconnectivity graphs? A large amount of calculations need to be performed before a database of viable structures can be created, and even then not all of those structures may be suitable for inclusion into the disconnectivity graph.

The answer is in the study of protein folding. This database and the disconnectivity graphs help in the study of the transitions between different forms of protein, however, we could also look at the transition between the two lowest minima of Lennard-Jones $N = 75$ (figure 11). In this case, which has the lowest energy barrier, there are 65 transition states between the two minima. The shortest possible path was $41.5\,\sigma$ but involved a much higher barrier.

V. BASIN HOPPING

If I've got enough time I would like to talk about basin hopping [4], which is the method used by David Wales' group to create the database of structures used in the creation of the disconnectivity graphs shown in this handout. The PES is transformed by using equation 1.

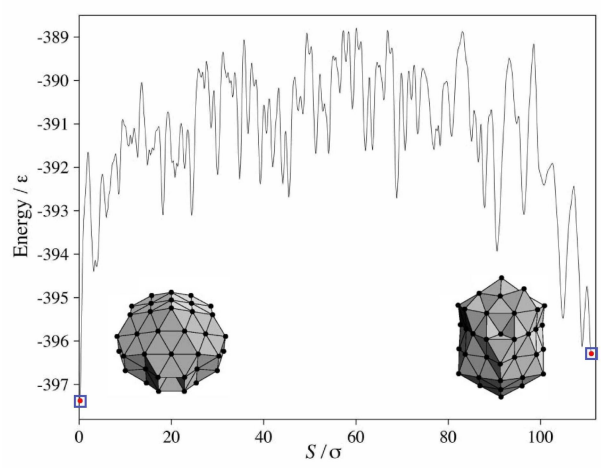

FIG. 11: Graph showing the transition between the two lowest forms of L_{J75}. S is a measure of the path length between structures [1].

$$\tilde{\mathrm{E}}_c\left(\mathbf{X}\right) = \min\{\mathrm{E}_c\left(\mathbf{X}\right)\} \tag{1}$$

This has the effect of reducing the search space into a series of staircases, where the plateaus correspond to minima (figure 12).

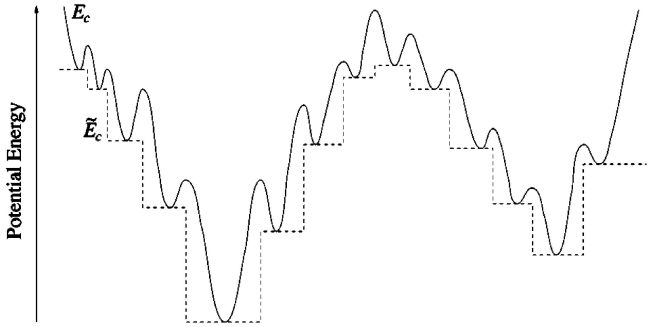

FIG. 12: Schematic diagram for basin hopping [5]

This transformation does not change the identity of the global minimum, or the relative energies of any of the minima.

The landscape is explored using a canonical Monte Carlo simulation at a constant temperature. At each step the coordinates are displaced by a random number in the range [-1,1] times the step size, which due to the nature of this transformed surface, can be relatively large. It was adjusted to give and acceptance ratio of 0.5. A Polak-Ribiere conjugate gradient minimisation is used to transform the PES as described by 1. More information on this algorithm can be found in reference [5].

Applying this algorithm to the LJ_{38} cluster gives the dissconectivity graph in figure 13.

The funnel nature of the icosahedral part of the graph is

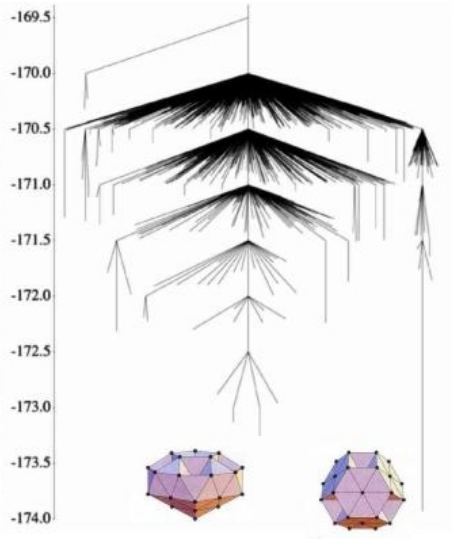

FIG. 13: LJ_{38} with basin hopping [1]

even more evident, and now appears similar to the ideal funnel for LJ_{13} from figure 4, while the funnel down to the global minimum is even more obvious.

VI. CONCLUSIONS

I hope I have been able to demonstrate the usefulness of disconnectivity graphs in giving a visual description of a multi-dimensional energy landscape. These can also be applied to large number of different systems with great effect.

Basin hopping transforms the PES in a way that removes downhill barriers and as such improves the determination of the global minimum and local minima. The basin hopping algorithm, when combined with disconnectivity graphs, can also help gain a deeper understanding of the problem.

[1] J. P. K. Doye, M. A. Miller, and D. J. Wales. Evolution of the potential energy surface with size for lennard-jones clusters. *J. Chem. Phys.*, 111:8417–8428, 1999.

[2] D. A. Evans and D. J. Wales. Free energy landscapes of model peptides and proteins. *J. Chem. Phys.*, 118:3891–3897, 2003.

[3] T. F. Middleton and D. J. Wales. Energy landscapes of some model glass formers. *Phys. Rev. B*, 6402:art. no.–024205, 2001.

[4] D. J. Wales and J. P. K. Doye. Global optimization by basin-hopping and the lowest energy structures of lennard-jones clusters containing up to 110 atoms. *J. Phys. Chem. A*, 101:5111–5116, 1997.

[5] David J. Wales. Energy landscapes: With applications to clusters, biomolecules and glasses. *Cambridge University Press*, ISBN 0-521-814157-4, 2003.